COMBUSTION OF A HIGHLY MOIST BIOMASS PARTICLE IN A FLUIDIZED BED

دراسة احتراق كريات من الوقود الحيوي عالي الرطوبة في فرن مهد مميع

F. OKASHA

Lecturer, Mechanical Eng. Dept, Faculty of Engineering, Mansoura University.

خلاصة :

تعد المخلفات الحيوية إحدى تحديات البيئة النظيفة، إلا أن الكثير منها يمكن اعتباره من الطاقـــات المتجـــددة إن أحســـن توظيفها. و تعد تكنولوجيا المهد المميع إحدى أهم البدائل للاستفادة من طاقة المخلفات الحيوية إما بالحرق المباشر أو بتحويلها إلى غـاز. ولتحقيق كفاءة عالية للاحتراق وتقليل الإنبعاثات الضارة يكون من الأهمية بمكان معرفة تفاصيل آلية الإحراقات الحرارية المختلفة الـتي تمر بها كريات الوقود الحيوي عند احتراقها. وقد استهدف هذا البحث عمل دراسة تحليلية و عملية للإحراقات الحرارية المختلفة الـتي تمر بها كرية من الوقود الحيوي عالي الرطوبة داخل فرن ذا مهد مميع (جفاف الرطوبة- التحلل الحراري وانبعاث المـــواد الطيـــارة – احتراق الكربون الثابت). وقد تناولت الدراسة ثلاثة أنواع مختلفة من الوقود الحيوي وتشمل تفل قصب السكر وروث الماشية و مـــاق نبات روبينيا. وقد تناولت الدراسة قياس و حساب الزمن اللازم للتحلل الحراري وانبعاث المواد الطيارة وكذلك الزمن اللازم لاحـتراق الكربون المتبقي مع دراسة تأثير مختلف ظروف التشغيل وخصائص الوقود عليهما. وقد وجد توافق جيد بين النـتائج العمليـة وتلـك التحليلية. وقد تم استنتاج ثوابت خاصة بآلية التحلل الحراري واحتراق الكربون المتبقي لهذه المواد الحيوية والتي من المرجو أن تكـــون مفيدة عند عمل تنبؤات أو نماذج رياضية.

ABSTRACT

Drying, devolatilization and char combustion of a single highly wet biomass particle in a fluidized bed has been studied. In the present work three different biomass fuels are considered including bagasse, manure and robinia. An experimental program has been carried out using a bench scale fluidized bed combustor. The combustor is made of quartz glass, which is electrically heated. Duration of volatiles release and that of char combustion have been recorded by nicked eye and gas analysis. The effect of operating parameters (bed temperature, fuel particle size, oxygen concentration) and particle characteristics has been investigated. A simplified mathematical model of heat-transfer controlled pyrolysis has been developed to understand the experimental data. The model predictions are in a good agreement with the experimental results. The model can be used to estimate the devolatilization times in other combustion systems. Kinetic parameters of char combustion are obtained, based on the measured burnout times and simple model considerations.

KEYWORDS

Fluidized Bed-Biomass-Combustion-Drying-Devolatilization

1. INTRODUCTION

Amongst the renewable energies, biomass is expected to be one of the most important in the near future. Indeed, biomass is a renewable fuel, which can be burnt or gasified similarly to other fossil fuels, using the same technologies with special adaptations. If similar to conventional fossil fuels, it is different in its composition, its LHV, and its corrosivity. A remarkable asset is its comparatively low impact on the environment; the content in N and S being very low, so are the emissions of NO_x and of SO_2. Moreover, use of biomass fuels saves the diminishing fossil fuels and

Accepted May 19, 2001

alleviates the growing waste disposal problem. On top of that, biomass has a zero CO_2 balance on a period of a few years. On the other hand, governments commit themselves to reduce their CO_2 emissions in the international meetings about the Global Climate Change like in Kyoto (1997), Buenos Aires (1998). In this framework the use of biomass in power generation is promoted [Mathieu and Dubuisson, 1999].

In the last decade, many new biomass power plants have been built and the development of new technologies for biomass based power generation is proceeding. Among these technologies, fluidized bed combustion (FBC) is an important process for utility-scale biomass power plants, due to its high combustion efficiency, low emission level and good fuel flexibility [Weigang Lin and Kim, 1999]

Although fluidized bed combustion (FBC) technique is the most promising in this respect, the designs of existing fluidized bed boilers and gasifiers are mainly based on experience from coal combustion. The expanding applications of fluidized bed combustion in conjunction with the use of biomass call for thorough reconsideration of the role of fundamental processes like fuel drying, devolatilization, volatile mixing and combustion. These processes are relevant to the achievement of substantial combustion efficiencies and of uniformity temperature profiles in the combustor, to preventing pollutant formation and to establishing efficient reactor control strategies.

Many types of biofuels have high moisture content, up to 80% and volatile matter up to 50%. For this type of fuel, drying and devolatilization of the particles are the main stages of combustion, since fixed carbon content is only small ratio. Literature on drying, devolatilization and combustion mechanisms of coal type fuels in fluidized beds is vast (see for example Agarwal and La Nauze, 1989). So far there is practically little information available on the kinetics of biofuels combustion. The present paper presents an experimental study and a theoretical analysis of devolatilization and char combustion of a single particle in fluidized bed. Given that FBC of a single particle provides well-defined boundary conditions, the data obtained can be applied to other combustor types by means of the similarity approach.

2. EXPERIMENTAL

2.1. Test Rig

The experiments have been carried out using a bench scale fluidized bed reactor FBR-40, Fig. 1. It consists of two main sections separated by a distributor plate. The lower section, made of steel, operates as an air pre-heater. The higher one is the fluidizing column made of quartz tube, 40 mm in diameter. The transparent walls of the column permit visual observation of the reactor during the operation. Two semi-cylindrical radiant shells are installed around the two sections of the unit. To make possible visual observation inside the fluidized column, two facing spaces are kept between the two shells. The electric furnace supplies the required power for both of preheating section and fluidization column in order to maintain the bed at operating temperature. A cooled probe is inserted from the top of the quartz tube to allow gas sampling. The bed temperature is regulated by means of a PID electronic controller connected to a thermocouple inserted just above the distributor plate. Silica sand with a narrow size distribution (0.60-0.85 mm) has been used as bed material. Its experimental minimum fluidization velocity is 23 cm/s at 850 °C.

2.2 Experimental Procedure

A single fuel particle of initial diameter d_{po}=2-20 mm is fed over the fluidized bed at steady state conditions. The delay period before volatile ignition, t_{vd}, volatile flaming period, t_{vf} and the char burnout time, t_c have been recorded by visual observation. The concentrations of CO, CO_2, total hydrocarbons of the flue gases are monitored and recorded by using a personal computer equipped with a data acquisition unit. Series of experiments are carried nut in oxidising environment until complete combustion.

To investigate mass loss history a number of eqnal fuel particles are fed and retrieved out the bed after different time intervals and quenched with cold nitrogen to interrupt oxidation. Then, the particle is weighed to obtain the mass loss.

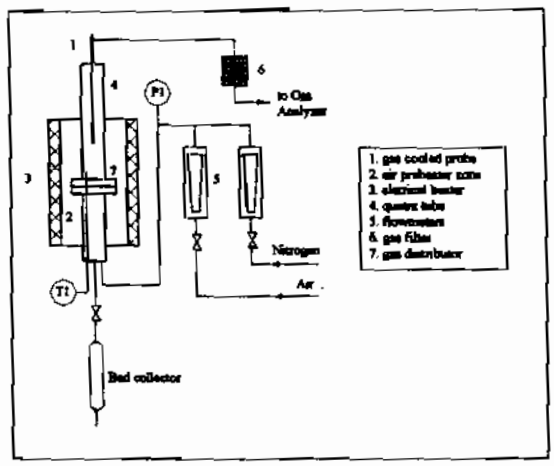

Figure 1. Experimental Apparatus FBR-40

Three types nf biomass fuel are studied. Table 1 reports the properties of raw fuels considered in the present work.

Fuel	Bagasse, B	Manure,M	Robinia, R
Proximate Analysis (as received)			
Moisture, %	46	42	32
Volatile matter, %	45	36	55
Fixed carbon, %	7	5	12
Ash, %	2	17	1
Ultimate Analysis (dry basis)			
Carbon, %	48.8	36.8	43.42
Hydrogen, %	5.8	4.5	7.70
Nitrogen, %	0.21	2.8	0.02
Sulphur, %	-	0.6	-
Oxygen, %	41.7	26	47.62
Ash	3.5	29.3	1.23
Density, kg/m^3	490	570	380
Lower calorific value, kcal/kg	2610	2122	3560

Table 1. Biofuels properties and analysis

3. MODELLING

3.1. Heat and Mass Transfer Characteristics

Heat and mass transfer coefficients to/from a particle immersed in a fluidized bed are estimated as recommended by Leckner et al. (1992). The overall heat transfer coefficient is a sum of convective and radiative constituents.

$$h_m=(D/d_i)[(Sh_l-Sh_a)(d_i/d_p)^{2/3}+Sh_a] \quad (1)$$

$$Sh_l = 2\varepsilon_{mf} + 0.117 Ar_i^{0.39} Sc^{1/3}$$

$$Sh_a = 0.009 Ar_i^{1/2} Sc^{1/3}$$

$$h = h_c + h_r \quad (2)$$

$$h_c = (k_g / d_i)[(Nu_l - Nu_a)(d_i / d_p)^{2/3} + Nu_a] \quad (3)$$

$$Nu_l = 6 + 0.117 Ar_i^{0.39} Pr^{1/3}$$

$$Nu_a = 0.85 Ar_i^{0.19} + 0.006 Ar_i^{1/2} Pr^{1/3}$$

$$h_r = \sigma(T_b^2 + T_a^2)(T_b + T_a)/(1/\varepsilon_b + 1/\varepsilon_a - 1) \quad (4)$$

The emissivity is chosen to be ε_a=0.9 for the fuel particle and ε_b=0.8 for the fluidized bed.

In the present work the thermal conductivity of dry biomass particles is estimated by the empirical formula of MacLean (1941).

$$k_c = 0.0237 + 0.0002\rho_d \quad (5)$$

The external temperature of the char layer quickly reaches a temperature close to the bed temperature around 1100 K. At such a temperature, a radiative thermal conductivity, k_r, should provide an essential input. Accounting for a high porosity of char, up to ε_v=0.9 for biomass char, a model of Pavlyukevich (1990) for radiation in a highly porous material can be used to estimate k_r.

$$k_r = 4(\varepsilon_v/(1-\varepsilon_v))\sigma d_{pore} T_c^3 \quad (6)$$

$$k = k_c + k_r \quad (7)$$

T_b is chosen as a reference temperature for the physical properties of gas (air) as well as for the diffusion coefficient of oxygen in air, D. The latter is estimated by the modified Sutherland's formula, Pomerantsev et al. (1986)

$$D = D_o\left(\frac{(C_1+273)(C_2+273)}{(C_1+T_b)(C_2+T_b)}\right)^{1/2}\left(\frac{T_b}{273}\right)^{5/2} \quad (8)$$

where D_o=17.8 10^{-6} m^2/s, C_1=115, C_2=138.

3.2. Drying and Devolatilization

In this study the shrinking core model is adopted to drying of highly wet biomass particle under FBC. Agarwal and LaNauze (1989) adopted the model to a coal particle of different shapes.

Let us take into consideration a highly moist biomass particle fed into FBC. Once the particle surface reaches the boiling temperature the drying process starts at the receding surface of the wet core. The temperature at the wet-dry interface remains constant, the receding rate being heat transfer controlled. As the drying proceeds, the particle surface reaches the temperature at which devolatilization initiates. An abrupt pyrolysis is considered to occur at the receding char-dry interface once its temperature

reaches the upper limit of pyrolysis range, T_v. After that, the pyrolysis front continuously advances toward the centre of the particle, since the thermal wave follows the wet-dry interface. Thus, the drying and pyrolysis of a biomass particle can be considered as a coupled process with heat transfer as the controlling mechanism (Agarwal and La Nauze, 1989).

The model can be solved analytically under a pseudo-steady state simplification. A pseudo-steady state approximation means that time of thermal conduction through the dry shell of a thickness δ, $t_c \propto \rho_d c_p \delta^2 / k_d$ is small compared to the characteristies receding time of the wet-dry interface of a radius r_{wc}, $t_{wc} \propto q\rho_{wc} W_o r_{wc}^2 / k_d (T_b - T_{wc})$, and the distribution of temperature over the thickness of the dry shell is that of steady state condition.

3.2.1. Model assumptions

1. Fuel particles are isotropic and homogeneous and have constant size.
2. All moisture content is free water.
3. The drying occurs at the receding surface of the wet core, since the rate of the process is heat transfer controlled.
4. An abrupt pyrolysis occurs when the dry shell locally reaches a characteristic pyrolysis temperature, T_v. The latter is corresponding to the higher limit of the temperature range of devolatilization of biomass.
5. The temperature distributions in the outer char shell and in the intermediate dry layer are those of a steady state condition.
6. The temperature of the wet-dry interface, T_{wc}, remains constant at the saturation temperature. For simplicity, the initial temperature of the particle is equal to T_{wc}.
7. The water vapor and pyrolysis gases do not affect the heat transfer because of the existence of cracks, and no mass transfer effect is considered for the same reason.

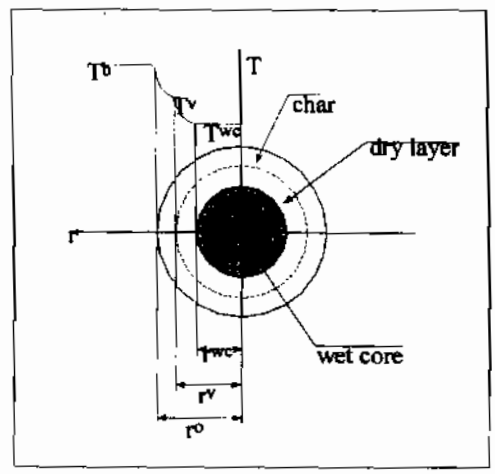

Figure 2. Different zones inside a biofuel particle during drying and devolatilization.

3.2.2. Mathematically

The energy balance for a spherical fuel particle is given by:

$$\frac{1}{r^2}\frac{\partial}{\partial}\left[r^2\frac{\partial T}{\partial r}\right]=\frac{1}{\alpha}\frac{\partial T}{\partial t} \tag{9}$$

For a pseudo state approximation the equation is reduced to

$$\frac{1}{r^2}\frac{\partial}{\partial}\left[r^2\frac{\partial T}{\partial r}\right]=0 \tag{10}$$

The equation may be put in dimentionless form

$$\frac{1}{R^2}\frac{\partial}{\partial}\left[R^2\frac{\partial \theta}{\partial R}\right]=0 \tag{11}$$

where $R=\frac{r}{r_o}$ r_o is the initial diameter of biomass particle

$\theta=\theta_c=(T-T_v)/(T_b-T_v)$ $r_o<r<r_v$

$\theta=\theta_d=(T-T_{wc})/(T_b-T_{wc})$ $r_v<r<r_{wc}$

Initial condition

$$\theta|_{\tau=0}=\theta_{wc} \tag{12}$$

Boundary conditions

-at the surface of the particle

$$\left.\frac{d\theta}{dR}\right|_{R=1}=Bi(1-\theta_s) \tag{13}$$

This condition holds for dry biomass until the surface temperature reaches T_v, $t<t_{vd}$, and for char after this instant, $t_{vd}<t<t_{vf}$;

- at the wet-dry interface

$$\theta_d|_{R_{wc}}=0 \tag{14}$$

$$\left.\frac{d\theta_d}{dR}\right|_{R_{wc}}=-\frac{dR_{wc}}{d\tau} \tag{15}$$

- at the char-dry biomass interface

$$Z\left.\frac{d\theta_c}{dR}\right|_{R_v}=\left.\frac{d\theta_d}{dR}\right|_{R_v} \tag{16}$$

where $Z=k_c(T_b-T_v)/k_d(T_b-T_{wc})$

Analytical solution of the model can be obtained provided that all thermal properties in the equations are constant with time. After many mathematical manipulations, the following expressions can be derived

Temperature distribution before starting of pyrolysis

$$\theta=\frac{R-R_{wc}}{R(1-B_dR_{wc})} \tag{17}$$

Wet core radius at beginning of devolatilization at surface of the particle

$$R_{wc,o}=\frac{1-\theta_v}{1-B_d\theta_v} \tag{18}$$

Delay period before starting of devolatilization (first period of drying)

$$\tau_1=\tau_{vd}=\frac{1}{2}\left(1-R_{wc,o}^2\right)-\frac{B_d}{3}\left(1-R_{wc\,o}^3\right) \tag{19}$$

Temperature distribution through char layer

$$\theta_c = \frac{R - R_v}{R(1 - B_c R_v)} \quad (20)$$

Temperature distribution through dry layer

$$\theta_d = \frac{(\theta_v + Z)(R - R_{wc})}{R(1 - R_{wc} B_c)} \quad (21)$$

devolatilized radius

$$R_v = \frac{R_{wc}(\theta_v + Z)}{Z + \theta_v R_{wc} B_c} \quad (22)$$

Time required for shrinking wet core, R_{wc}, after beginning of devolatilization

$$\tau = \frac{1}{\theta_v + Z}\left[\frac{1}{2}\left(R_{wc,o}^2 - R_{wc}^2\right) - \frac{B_c}{3}\left(R_{wc,o}^3 - R_{wc}^3\right)\right] \quad (23)$$

where $\tau = t/t_o$ and $t_o = q\rho_o W_o r_o^2 / k_d (T_b - T_{wc})$

Time required for complete drying of the particle after beginning of devolatilization (the second period of drying)

$$\tau_2 = \tau_{vf} = R_{wc,o}^2 (3 - 2B_c R_{wc,o}) / 6(\theta_v + Z) \quad (24)$$

Total time of particle drying

$$\tau_d = \tau_1 + \tau_2 \quad (25)$$

3.3. Char Combustion

Usually the biomass fuel particles are larger than 1 mm. So the chemical reaction of the fixed carbon is assumed to result in carbon dioxide. This assumption is in accordance with the results found by Ross and Davidson (1981).

$$C + O_2 \rightarrow CO_2 \quad (26)$$

The mass balance for a spherical particle burning following shrinking sphere model has the form

$$\frac{d}{dt}\left(\frac{\pi d_p^3}{6}\rho_{po} C_f\right) = -\mu k_{ov} C_{O2} \pi d_p^2 \quad (27)$$

The overall reaction rate coefficient k_{ov} can be expressed through the diffusion and kinetic resistance

$$\frac{1}{k_{ov}} = \frac{1}{h_m} + \frac{1}{k_c} \quad (28)$$

Assuming that μ and C_{O2} remain unchanged in the combustion process and integrating Eq. (28) between t=0 and char burn-out time t_c, the following expression estimate the average overall reaction rate coefficient,

$$k_{ov} = \frac{1}{2}\frac{\rho_{po} C_{fc} d_{po}}{\mu t_c C_{O2}} \quad (29)$$

One can estimate the chemical reaction rate constant k_c from the expression (28).

The temperature of burning particle can be estimated by the following expression, see Leckner et al. (1992)

$$T_p / T_b = 0.84 Ar_i^{0.05} \quad (30)$$

4. RESULTS AND DISCUSSION

The delay period of volatiles ignition time, t_{vd}, the flaming period of volatiles or volatiles release duration, t_{vf}, and the particle-char burnout time, t_c, have been visually observed and recorded. The state of a burning particle could be easily traced. During devolatilization it was mostly floating on the surface of the bed because of an intensive outflow of vapour and gas. The particle kept its shape and decreased insignificantly in size during this stage. The devolatilized and ignited char residues looked bright light on the darker background of the bed and were gradually decreasing in size. The char particles circulated within the bed, periodically rising to the surface. Some fines, probably ashes, were split off the char particle. Finally the particle crumbled into a number of sparkles and got lost out of view. At that moment the burnout time was registered.

Progress of drying and devolatilization throughout the particle layers are studied. The volume of dried layers, $V_d(t)$ and that of devolatilized layers, $V_v(t)$ are calculated as a function of time along the drying period. The ratio of $V_v(t)$ to $V_d(t)$ is used to express the lag between devolatilization and drying processes. Figure 3 represents the ratio as a function of time at various Biot numbers. It is noted that the lag between the beginning of devolatilization and beginning of drying decreases as the Biot number increases. For typical conditions, Bi=10 to 50, the lag is practically absent. The effect of the Biot number becomes insignificant at Bi>50. At the end of the drying period, the ratio is close to 1 for Biot number greater than 2. Thus the end of devolatilization of the particle coincides with the end of drying under typical conditions of FBC.

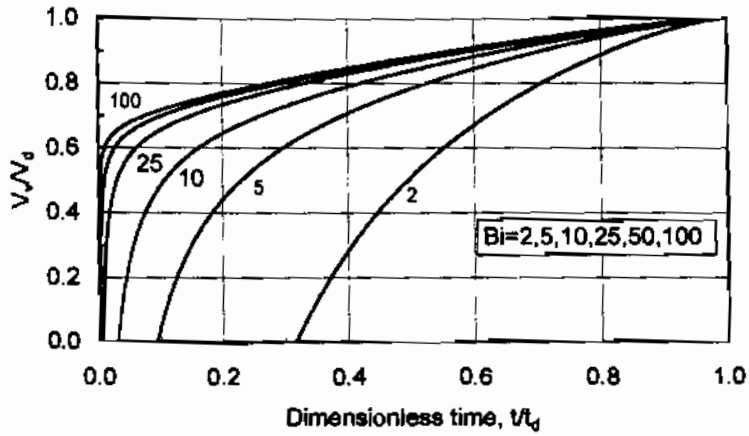

Figure 3. Ratio between volume of devolatilized layers to that of dried Layers as a function of time, at various Biot numbers.

A typical mass loss history of spherical particles of Bagasse is shown in Fig. 4. There is a good agreement between the experimental data and the calculated results.

A comparison between model results and experimental devolatilization time is presented versus the initial particle diameter in Fig. 5, for the three biofuels. Effect of moisture content is obvious. The biofuel with higher moisture content requires longer release volatile period. Bagasse has higher moisture content and requires longer volatile release period compared to robinia. On the other hand bagasse has shorter release volatile period than that of manure although bagasse has higher moisture

content. This later should be ascribed to the ash eontent of manure (17%) compare to bagasse (2%). Existence of high ash content makes the char less porous with smaller pore diameter. Thus the radiative thermal conductivity decreases. Consequently, The heat transfer rate through the particle layers is reduced making the release period of volatile longer.

The volatiles release-time can be described by empirical power-law correlations, normally used in the literature

$$t_v = k_v d_p^n \qquad (31)$$

with the parameters, k_v and n, shown in Table 2. The correlation (31) can be applied to conditions similar to those studied in the present paper.

	Bagasse	Manure	Robinia
k_v	0.577	0.624	0.42
n	1.85	1.87	1.84

Table 2. Experimental kinetic parameters of devolatilization

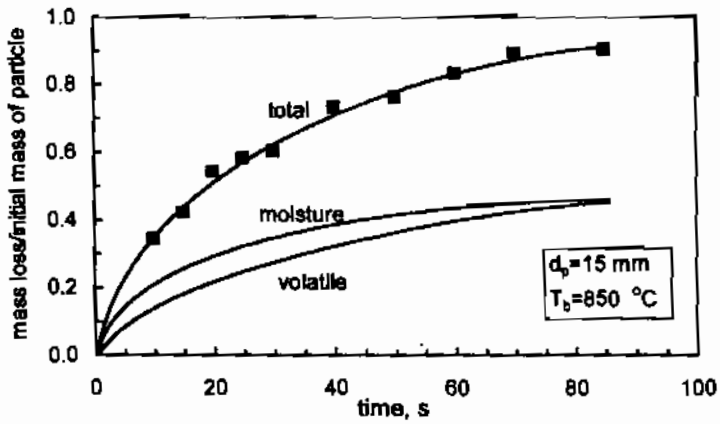

Figure 4. Mass loss histories of bagasse particle

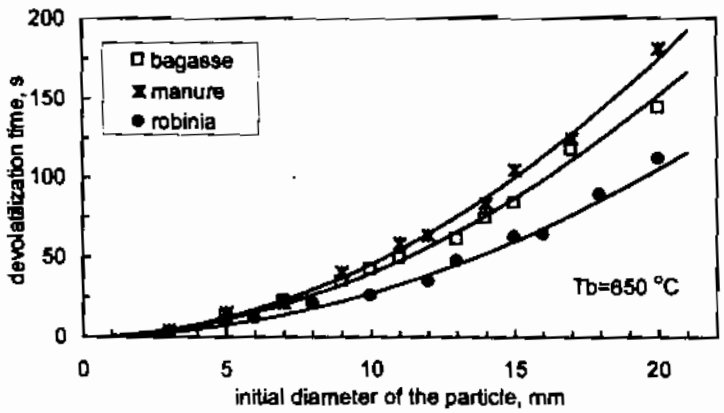

Figure 5. Comparison between experimental (symbols) and calculated (lines) volatiles release times.

The effect of bed temperature on volatile release time is shown in Fig. 6. As expected increasing bed temperature reduces the volatile release period due to increase of heat transfer rate especially by radiation.

Figure 7 represents the influence of moisture content on the volatile release period. These results could be useful for designer to choose the suitable moisture content that gives optimum combustor performance when pre-drying of biofuel is necessary.

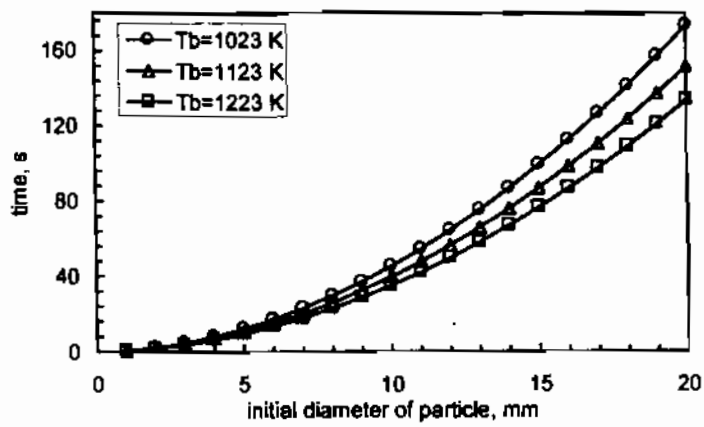

Figure 6. Influence of temperature on volatile release time.

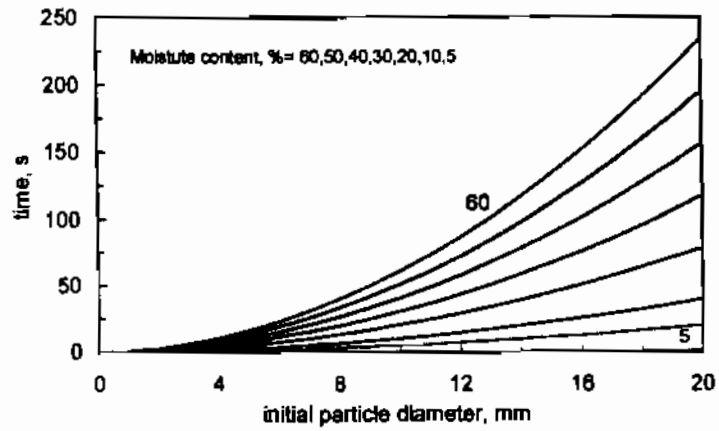

Figure 7. Effect of moisture content on volatile release time.

The Experimental overall reaction rate constant, k_{ov} evaluated by Eq. 29 is shown in Figure 8. In this figure time-average values of external mass transfer coefficients of burning particles are plotted for comparison. The time average value is obtained by integration of Eq. 1. The average chemical reaction rate constant, k_c, is estimated by Eq. (28) with k_{ov} and h_m known. At bed temperature of 850 °C the average value of k_c is found to be around 0.5, 0.2, 0.65 m/s for bagasse, manure and robinia, respectively. The low value of k_c for manure may be ascribed to its high ash content.

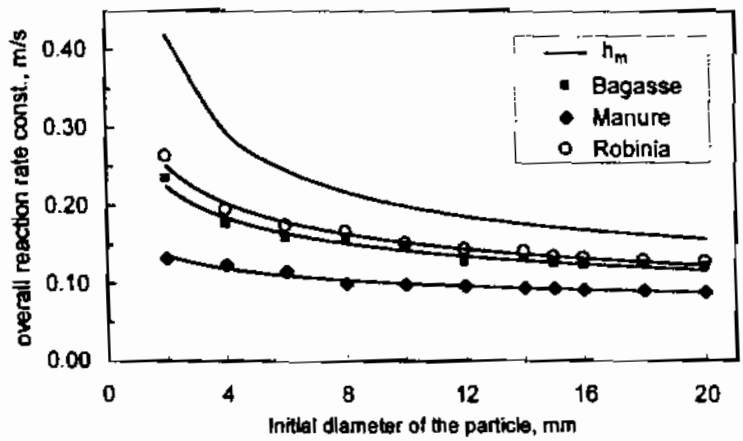

Figure 8. Experimental overall reaction rate constant at T_b=1123 K.

Figure 9 shows the char burning time as a function of initial particle diameter for the three fuels. The char burning time is estimated by Eq. 28 using k_c obtained from the experimental data. According to Eq. 28 char burning time directly increases with particle diameter. In addition, overall reaction rate constant, k_{ov} is dependent on particle diameter. k_{ov} significantly reduces with particle diameter at small diameter range and reduces slightly at large diameter, see Fig. 8. The later reason results in a more increment in time burning of char especially at small diameter. In Fig. 9 it is also noted that the burning time of char is close for the three biofuels. The explanation of this result is that the char of fuel type with higher overall reaction rate constant has higher fixed carbon content, see table 1 and Fig. 8.

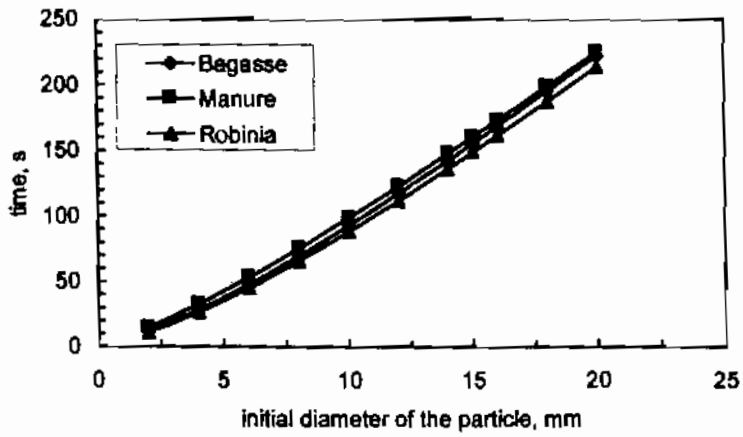

Figure 9. Char burning time as a function of initial particle diameter.

Figure 10 represents experimental values of k_c in Arrhenius' coordinates, with the data being described by the global-kinetic expression,

$$k_c = A \exp(-E/RT) \qquad (32)$$

The obtained values of the activation energy, E and constant A are (48620 kJ/kmole, 35 m/s) (65140 kJ/kmole, 68 m/s) and (41528 kJ/kmole, 27 m/s) for bagasse, manure and robinia, respectively.

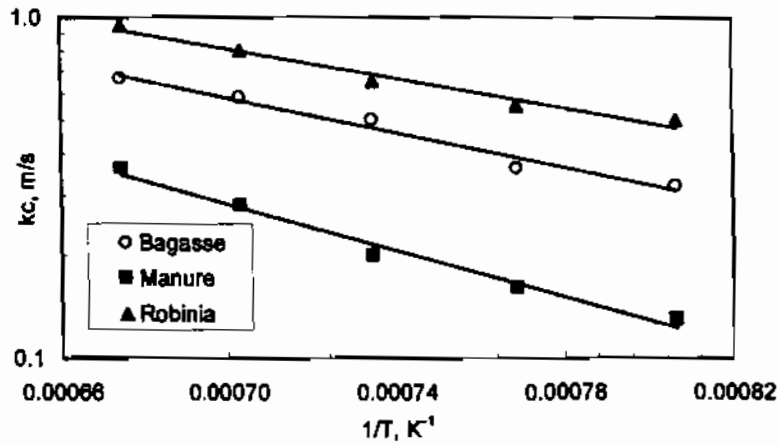

Figure 10 Arrhenius' representation of experimental data on char combustion

It can be shown for steady state combustion of mono-sized fuel that t_v/t_c is equal to the ratio of the number of devolatilized fuel particles to the number of char residues in the furnace. Experimental values of t_v/t_c are shown in Fig. 11. It is noted that t_v/t_c increases with the size of the fuel particles. Data shown in Fig. 11 are obtained at maximum oxygen concentration in the air, 21%. According to Eq. (29), the lower oxygen concentration the higher char burnout time, whereas volatiles release time practically does not change. Thus with lower oxygen concentration t_v/t_c should be reduces.

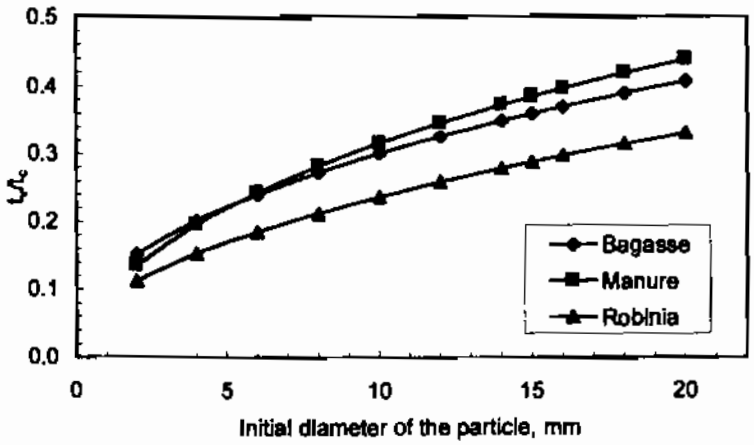

Figure 11. Ratio of volatile time to time of char combustion, at T_b=1123 K.

Table 3 compares the particle burnout times in a fluidized bed measured at an oxygen concentration of C_{02}=21 %, with predictions. There is a good agreement between predictions and experiments. The deviation is usually less than 5%.

Type	d_p	Model results			Experiment	deviation
	Mm	t_d, s	t_c, s	t_t, s	t_e, s	%
Bagasse	4	7.22	28.62	35.84	37	-3.13
	10	39.90	93.25	133.15	127	4.84
	15	86.83	155.56	242.39	254	-4.57
	20	151.63	222.34	373.97	385	-2.86
Manure	4	8.07	33.21	41.28	43	-4.00
	10	45.56	99.18	144.74	152	-4.78
	15	99.78	160.45	260.24	256	1.65
	20	151.63	225.06	376.69	390	-3.41
Robinia	4	4.81	26.60	31.41	33	-4.81
	10	27.32	88.56	115.88	121	-4.23
	15	59.94	148.79	208.74	199	4.89
	20	105.15	213.56	318.71	328	-2.83

Table 3. Particle total burn-out time, a comparison between model and experiments.

5. CONCLUSION

Mechanism of combustion of highly wet biomass is studied and investigated. New data is obtained on the different stages of combustion, drying, devolatilization and char combustion. According to the present work the following concluding remarks may be drawn.

1. Volatiles and water vapour are found to be yield simultaneously from the biofuel particle under FBC conditions.
2. The devolatilization time, t_v, decreases as expected with an increase of the particle diameter, the bed temperature, T_b, and decrease of moisture content
3. The char combustion time is higher with increase of both fixed carbon and ash content.
4. The ratio t_v/t_c increases with:
   - increase of the biomass particle diameter
   - increase of the oxygen concentration, since t_v is virtually independent of oxygen concentration.
5. A simplified analytical model of heat transfer controlled is established. The model describes well the experimental volatiles release. Empirical correlations (31) and (32) are obtained for the volatiles release time and kinetics of particle char combustion.

6. NOMENCLATURE

Ar_i Archimedes number of inert particle, $gd_i^3(\rho_i - \rho_g)/(\nu_g^2\rho_g)$

B_c $(Bi_c\text{-}1)/Bi_c$

B_d $(Bi_d\text{-}1)/Bi_d$

Bi_c Biot number, hr_o/k_c

Bi_d Biot number, hr_o/k_d

C_f fixed carbon content

C_{o2} oxygen concentration

c_p	specific heat capacity
D	diffusion coefficient of oxygen
d_i	diameter of inert (bed) particle
d_p	diameter of fuel particle
d_{po}	Initial diamc ter of fuel particle
d_{pore}	pore diameter
E	activation energy
g	acceleration of gravity
h	heat transfer coefficient
h_m	mass transfer coefficient
k	thermal conductivity
k_c	chemical reaction rate constant
k_{ov}	overall reaction rate coefficient
k_v	kinetic of devolatilization constant
Pr	Prandtl number, $\rho_g C_{pg} v_g / k_g$
q	latent heat of evaporation
R	dimensionless radial co-ordinate, r/r_o
r	radial co-ordinate
Sc	Schmidt number, vg/D
Sh	Sherwood number, $h_m d_p/D$
T_a	time-average surface temperature of a fuel particle
T_b	bed temperature
T_v	volatile release temperature
t_c	char burnout time
t_{vd}	delay period before volatile ignition
t_{vf}	volatile flaming (release) time
W_o	initial moisture content
Z	$k_c(T_b - T_v)/k_d(T_b - T_{wc})$

Greek symbols

α	Thermal diffusivity, $k/\rho c_p$
ε_a, ε_b	emissivity
ε_{mf}	bed voidage at minimum fluidization
ε_v	porosity
Nu	Nusselt number, hd_p/k_g
μ	stoichiometric coefficient, (kg carbon)/(kg oxygen)
ν	kinematic viscosity
ρ	density
τ	dimensionless time
θ	dimensionless temperature
θ_v	$(T_v-T_{wc})/(T_b-T_{wc})$
σ	Stefan-Boltzmann constant

Subscripts

a	active particle
b	bed
c	char combustion; convective; conductive
d	dry
g	gas

i	inert particle
o	initial
r	radiative
s	surface
v	devolatilized
vd	delay before devolatilization
vf	volatile flaming
wc	wet core

REFERENCES

1. Abdel-Hafez A. H., 1988, "Simplified Overall Rate Expression for Shrinking-Core Bituminous Char Combustion", Chem. Eng. Sc., Vol. 43, pp. 839-845.

2. Agarwal P. K., La Nauze R. D., 1989, "Transfer Processes Local to the Coal Particle: A Review of Drying Devolatilization, and Mass Transfer in Fluidized Bed Combustion", Chem. Eng. Res. Des., Vol. 67, pp. 457-480.

3. Alliston M. G., Prbst S. G., Wu S. and Edvardsson C. M., 1995, "Experience with the Combustion of Alternate Fuels in a CFB Pilot Plant", 13th, Int. FBC Conf., Orlando, Florida.

4. Annamalai K., Ibrahim M. Y., and Sweeten J. M., 1987, "Experimental Studies on Combustion of Cattle Manure in a Fluidized Bed Combustor", Journal of Energy Resources Technology, Transactions of the ASME, Vol. 109, pp. 49-57.

5. Bathia S.K., Perlmutter D.D., 1980, "A Random Pore Model for Fluid-Solid Reactions: I. Isothermal, Kinetic Control", AIChE J., Vol. 26, p. 179.

6. Leckner, B. Palchonok, G.I., Andersson, B. A., 1992, "Representation of heat and mass transfer of active particles", Presented at the IEA-FBC Mathematical Modeling Meeting, Turku, Finland.

7. MacLean, J.D., 1941, "Thermal conductivity of wood", Trans. Amer. Soc. of Heating and Ventilation Engineers, 47, pp. 323-354.

8. Masi S., Salatino P., and Senneca O., 1997, "Combustion Rates of Chars from High-Volatile Fuels for FBC Application', 14th Int. Conf. On FBC, Vol. 1, pp. 135-142.

9. Mathieu, P. and Dubuisson, R.,1999, " Performance Analysis of a Biomass Gasifier integrated in a Hat Cycle", 4th Int. Congress on Energy, Environment and Technological Innovation, Vol. 1, pp. 557-562, Rome, Italy.

10. Pavlyukevich, N.v., 1990, "Radiation Slip in a Highly Porous Material Layer", J. Eng. Phys., 59, 1284-1286.

10. Pomerantsev, V.V., Arefjev, K.M., Ahmedov, D.B., 1987, "Fundamentals of Practical Combustion Theory, ed. V.V. Pomerantsev, Energoatomizdat Publishing House, Leningrad (in Russian). ,

11. Ross, I. B. and Davidson, J.F., 1981, "The Combustion of Carbon Particles in a Fluidized Bed", Trans. Inst. Chem. Engng, Vol. 59, pp. 108-114.

12. Wartha C., Winter F. and Hofbauer H., 1996, "Advantages and Disadvantages of Biomass Fuels on a Fundamental Combustion Basis in Fluidized Beds", 9th Europ. Bioenergy Conf., Copenhagen, Denmark.

13. Weigang Lin and Kim Dam-Johansen, 1999, "Agglomeratiou in Fluidized Bed Combustion Of Biomass - Mechanisms And Co-Firing With Coal", Proceedings of the 15th International Conference on Fluidized Bed Combustion ,Paper No. FBC99-0120, Savannah, Georgia, May 16 - 19.